Spark plasma sintering and mechanical properties of compounds in TiB2-SiC pseudo-diagram

Marc Singlard, Nicolas Tessier-Doyen, Geoffroy Chevallier, Stéphane Oriol, Guiseppe Fiore, Bruno Vieille, Claude Estournès, Michel Vardelle, Sylvie Rossignol

Spark plasma sintering and mechanical properties of compounds in TiB_2-SiC pseudo-diagram

Marc Singlard[a,b], Nicolas Tessier-Doyen[a], Geoffroy Chevallier[c], Stéphane Oriol[b], Guiseppe Fiore[b], Bruno Vieille[b], Claude Estournès[c], Michel Vardelle[a], Sylvie Rossignol[a,*]

[a] Institut de Recherche sur les Céramiques, UMR 7315, 12 rue Atlantis, 87068 Limoges Cedex, France
[b] Centre National d'Etudes Spatiales, Direction des Lanceurs, 52 rue Jacques Hillairet, 75615 Paris Cedex, France
[c] CIRIMAT, Université de Toulouse, CNRS, Université Toulouse 3 Paul Sabatier, 118 route de Narbonne, 31062 Toulouse Cedex 9, France

A B S T R A C T

The influence of spark plasma sintering (SPS) parameters (temperature, time, pressure) and the role of particle size on densification, microstructure and mechanical properties of commercial additive-free TiB_2, SiC and composites thereof were studied by X-ray diffraction, scanning electron microscopy, the ultrasonic method and indentation. Three particle sizes of SiC and 2 of TiB_2 were processed. An optimal cycle was found for TiB_2 and SiC: 2000 °C, 3 min dwell time, and 100 MPa applied at 600 °C. The relative density of pure SiC increases linearly from 70% to 90% when the initial particle size decreases from 1.75 μm to 0.5 μm. Pure TiB_2 was densified up to 87%. Using 2.5 wt% SiC in TiB_2, the relative density increases to 97%. Young's modulus and the hardness of all samples were measured, with results discussed. The higher properties were obtained for additive-free TiB_2–5% SiC with a relative density of 97% and with the Young's modulus and Vickers hardness values being close to 378 GPa and 23 GPa, respectively.

1. Introduction

Non-oxide ceramics are highly interesting materials due to their outstanding properties at high temperature. The main compounds are carbides, borides and nitrides of transition metals of groups IV and V (Zr, Ti, Hf, Nb, Ta, V), in addition to other popular ceramics such as silicon carbide SiC. All these materials have a high melting point and hardness in common [1]. Silicon carbide presents interesting properties, especially good dimensional stability with high stiffness, low thermal expansion [2], and low creep rate (approximately 10^{-9} s^{-1} at 1600 °C and 110 MPa) [3,4]. Therefore, silicon carbide is a promising material for structural applications that require dimensional stability at high temperatures. Among borides, hafnium- and zirconium-diboride (HfB_2 and ZrB_2) are the preferred compounds for use at very high temperatures and in oxidizing atmospheres because their oxidation resistance is better than that of other borides [5]. HfB_2 and ZrB_2 are often mixed with SiC in order to limit grain growth and improve oxidizing resistance owing to the formation of a dense layer of silicon dioxide (SiO_2) [6]. However, titanium diboride TiB_2 presents both a lower creep rate at high temperature (10^{-10} s^{-1} at 1600 °C and 175 MPa) [7] than that of ZrB_2 (10^{-7} s^{-1} at 1600 °C and 110 MPa) [8] and HfB_2 (10^{-7} s^{-1} at 1500 °C and 100 MPa) [9] and a higher stiffness (560 GPa for TiB_2 [10], compared to 489 and 480 GPa for ZrB_2 [11] and HfB_2 [12], respectively). As a consequence, TiB_2 is a promising material for structural applications at high temperatures and in non-oxidizing atmospheres such as nuclear electric propulsion, as the operating gas is oxygen-free [13].

Titanium diboride presents poor sinterability due to its low self-diffusion coefficient, high melting point and strong covalent bonding [14]. Pure and dense TiB_2 cannot be obtained by pressureless sintering [15], and field-assisted sintering techniques such as spark plasma sintering (SPS) are required. SPS is a sintering method similar to hot pressing, but the sample is heated using a pulsed current, directly if it is a conductor or indirectly if it is not a conductor (in this case, the sample is heated by graphite tools) [16]. Compared to other sintering methods, SPS is faster in heating and in densification (on the order of a few minutes) and allows sintering of high-temperature ceramics while maintaining low grain growth [17]. A relative density up to 97.5% can be achieved with fine TiB_2 powders (1–2 μm) [18–20]. However, it appears that the densification rate drops dramatically with coarser grains, down to 80% for grains with a mean size of 5.7 μm [21]. The effect of the sintering temperature is not clear: increasing the temperature (from 1700 to 1900 °C) increases [18,21] or decreases [20] the relative density. It is supposed that an abnormal grain growth occurs at

those temperatures and inhibits densification [20]. However, in the case in which temperature has a positive effect on densification, grain growth occurs as well (3.2–8.1 μm [18] and 8.2–9.2 μm [21] for temperatures from 1600 °C to 1800 °C). Use of a sinter-aid is a way to improve the densification of titanium diboride. Silicon carbide is especially effective to improve densification and oxidation resistance of titanium diboride [22]. Amounts of SiC as low as 2.5 wt% are sufficient to ensure a significant improvement of relative density of TiB_2 [23]. Higher amounts of SiC are detrimental to high-temperature properties [24].

Silicon carbide can be densified by SPS, and generally, submicron powders are used [25,26]. For a 500 nm-sized powder, a densification rate of only 92% is achieved at 1850 °C [27]. When decreasing the size to the nanoscale, the densification kinetics are improved, and much more dense samples of up to 97.5% are obtained [26]. Yamamoto et al. [25] studied the consolidation by SPS of two nanometer-sized SiC powders: a commercial one and a homemade one. The commercial powder was poorly sintered (78%) while the homemade powder was near fully dense (99%) with the same operating conditions (1700 °C, 5 min, 40 MPa, vacuum). According to Yamamoto, the difference in the densification rates is due to a difference in the ordering of the homemade powder during the sintering process [25]. Depending on the SPS parameters, the dwell time can have either no effect [27] or a significant effect [28,29] on the relative density. Hayun et al. found that the dwell time had a strong effect, with a relative density of 89% for 1 min to 99% for 10 min [29]. In most of the published papers, the densification of only one powder is studied, and therefore, the effect of the initial particle size is not studied, whereas it is well known that the initial particle size is a key parameter to ensure high densification kinetics and mechanical properties.

Thus, the aim of this paper is to study the sinterability of SiC and TiB_2 powders of different particle sizes and of mixtures of the two. Initially, the densification by spark plasma sintering of commercial powders is studied, especially the influence of process parameters (temperature, time, pressure) on relative density. In a second experiment, mechanical properties (Young's modulus and hardness) of the produced pellets are measured, discussed and compared to the literature.

2. Materials and methods

Two commercial silicon carbide powders were used with a mean particle size of 1.75 μm (grade b-hp, Starck, oxygen < 1% by mass) and 0.5 μm (grade BF17, Starck, oxygen < 1.8% by mass), respectively, named 1.75SiC and 0.5SiC. According to the supplier's data, the composition of the two powders is 90% β SiC and 10% α SiC. In addition, a third homemade silicon carbide powder was used with a mean particle size of 1 μm. Two commercial titanium diboride powders were used with a mean particle size of 4.75 μm (grade D, Starck, oxygen < 1.1% in mass) and 3 μm (grade F, Starck, oxygen < 2.5% in mass), respectively, named 4.75TiB_2 and 3TiB_2.

Densifications were achieved on a SPS machine (Dr. Sinter SPS-632Lx, Fuji Electronic Industrial CO., LTD., Japan) available at Plateforme Nationale de Frittage Flash located at the Université Toulouse 3 Paul Sabatier. The powders were loaded into a graphite die with an inside diameter of 15 mm. The composite samples of TiB_2-SiC were homogenized in a mixing machine (Turbula) for 15 h before testing. A graphite sheet (PERMA-FOIL®Toyo Tanso) was inserted between the powder and the die/punches to avoid unwanted reactions and for easy removal of the samples from the die after the sintering stage. The amount of introduced powder was calculated in order to obtain pellets of 2 mm in thickness at maximum densification. All experiments were conducted under vacuum (30 Pa). The temperature was first raised to 600 °C and maintained for 3 min to stabilize its reading with a pyrometer, and then, a heating ramp of 100 °C/min was applied up to the setpoint temperature. The pressure was initially set to 0.1 kN (0.6 MPa) to ensure electrical contact. After that, the final pressure was applied (i) at 600 °C (samples marked with an "H") or (ii) at the maximum temperature (samples marked with a "D"). After a dwell time of 3–20 min, the pressure was released and the current cut off.

To make reading this paper easier, the samples were tagged as follows:

particle[*phase*]

For example, $0.5SiC_{100H}^{2000;3}$ is a silicon carbide with an initial mean particle size of 0.5 μm processed by SPS at 2000 °C for 3 min with a pressure of 100 MPa applied from 600 °C.

The density of samples was measured by Archimedes' method using a hydrostatic balance (Sartorius MSE224S-YDK03). The relative density was calculated using a theoretical density of 3.21 g/cm^3 and 4.52 g/cm^3 for SiC and TiB_2, respectively [30]. For the composite samples, the rule of mixtures was used to determine the theoretical density.

Phases were analyzed by X-ray Diffraction XRD (D8 advance, Brüker) from 25° to 95° (2θ) in 0.015 steps.

Morphology observations were carried out with a scanning electron microscope (SEM) (IT300, JEOL). Before the observations, the pellets were polished and metallized with platinum.

Young's moduli were measured using the ultrasonic method [31] by reflection according to Eq. (1):

$$E = \rho \frac{3v_L^2 - 4v_T^2}{\frac{v_L^2}{v_T^2} - 1} \quad (1)$$

where E is Young's modulus (Pa), ρ is the apparent density of the pellet (kg/m^3), and v_L and v_T are the velocities of the waves in longitudinal and transverse modes, respectively (m/s). An ultrasonic coupling agent was used to ensure a good wave propagation. Vickers microhardness was measured using a diamond indenter under a load of 1 kg applied over 15 s. For each sample, the given hardness value was taken as an average of 10 measurements.

3. Results and discussions

3.1. Densification process of SiC

Fig. 1 shows the relative density of 1.75SiC processed with different SPS parameters. High temperature (2000 °C), pressure (113 MPa) or long dwell time (20 min) did not create samples with a high relative density, with the highest density being 70%. With a lower temperature (1900 °C instead of 2000 °C), the relative density became lower (60% instead of 70%), even with a longer dwell time (Fig. 1), which means that the onset of sintering was higher than 1900 °C for the 1.75SiC powder.

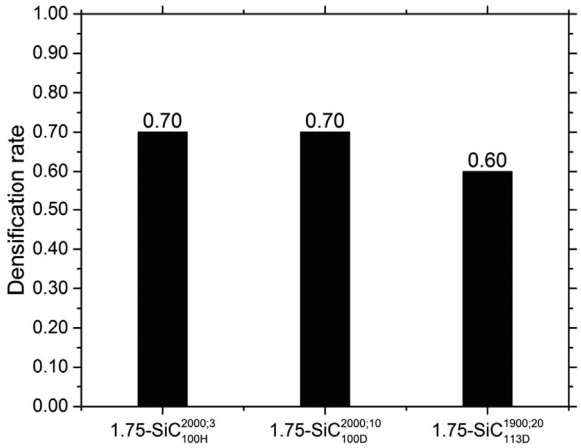

Fig. 1. Relative density of 1.75SiC processed with different SPS parameters.

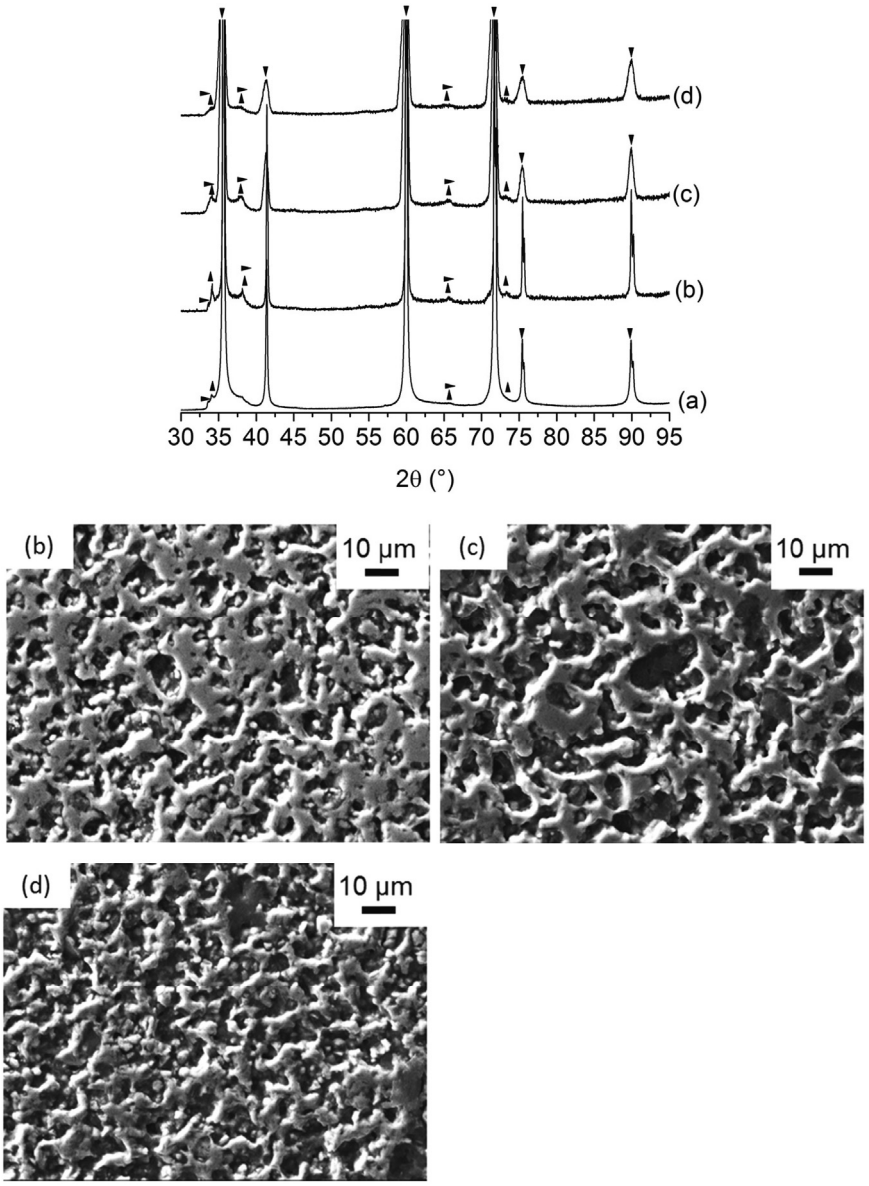

Fig. 2. XRD analyses and SEM observations of 1.75SiC. (a) raw powder, (b) $1.75SiC_{100H}^{2000;3}$, (c) $1.75SiC_{100D}^{2000;10}$ and (d) $1.75SiC_{100D}^{1900;20}$. ▼ SiC (3C) (PDF 029-1129), ▲ SiC (6H) (PDF 049-1428) and ► SiC (2H) (PDF 029-1126).

Fig. 2 shows the structural analysis of the pellets, performed by XRD and SEM. The XRD of the initial powder (Fig. 2-a) shows a main phase of β-SiC (3C), and two minor phases of α-SiC (6H and 2H), in good agreement with the supplier's data. After sintering, these phases were maintained, and the XRD patterns do not reveal any phase change (Fig. 2b–d). SEM observations reveal that the grain size is slightly lower for $1.75SiC_{100D}^{1900;20}$ (Fig. 2-d) than that for the other samples, which corresponds to the sample with the lower temperature. Actually, the grain growth of SiC was mainly affected by temperature and dwell time and was not heavily affected by the obtained relative density [27].

Considering that the higher relative density obtained with 1.75SiC is only 70%, finer powder is required. Indeed, it is well known that the particle size is a key parameter for obtaining very high relative density. Two finest powders were densified with the SPS parameters $^{2000;3}_{100H}$ and Fig. 3-a presents the relative densities obtained. As expected, the process efficiency increases continuously when the particle size decreases. The relative density increases from 70% to 90% (a 29% increase) for a particle size from 1.75 µm to 0.5 µm. Since 0.5SiC is the powder that presents better densification kinetics, several SPS cycles were tested on this powder. Given that the onset of densification is above 1900 °C, maximum temperature was set at 2000 °C and the effect of pressure application procedure ("D" or "H") and dwell time are studied. Fig. 3-b shows the results in terms of relative density. From an initial SPS cycle using a pressure procedure "D" and a 3 min dwell time (Fig. 3-b, bottom left), increasing the dwell time to 15 min has no significant effect on relative density (76–78%). However, when the pressure is applied directly at 600 °C ("H" samples), a significant increase in relative density is measured, up to 90% with a dwell time of 3 min. Therefore, it appears that the effect of cold pressing ("H") is higher than the effect of creep due to pressure at high temperature ("D") on grain rearrangement. Thus, dwell time has no effect on relative density, and it is better to use the "H" procedure. Fig. 3-c presents the densification kinetics (punch displacement) measured during the SPS process for 0.5SiC processed with different SPS parameters. At temperatures below 1500 °C (approximately 420 s in Fig. 3-c), the densification does not occur, and the samples expand due to thermal dilatation. At higher temperatures, the densification begins, and compaction is visible on the curves (Fig. 3-c). During the dwell time, the displacement is nearly constant, which

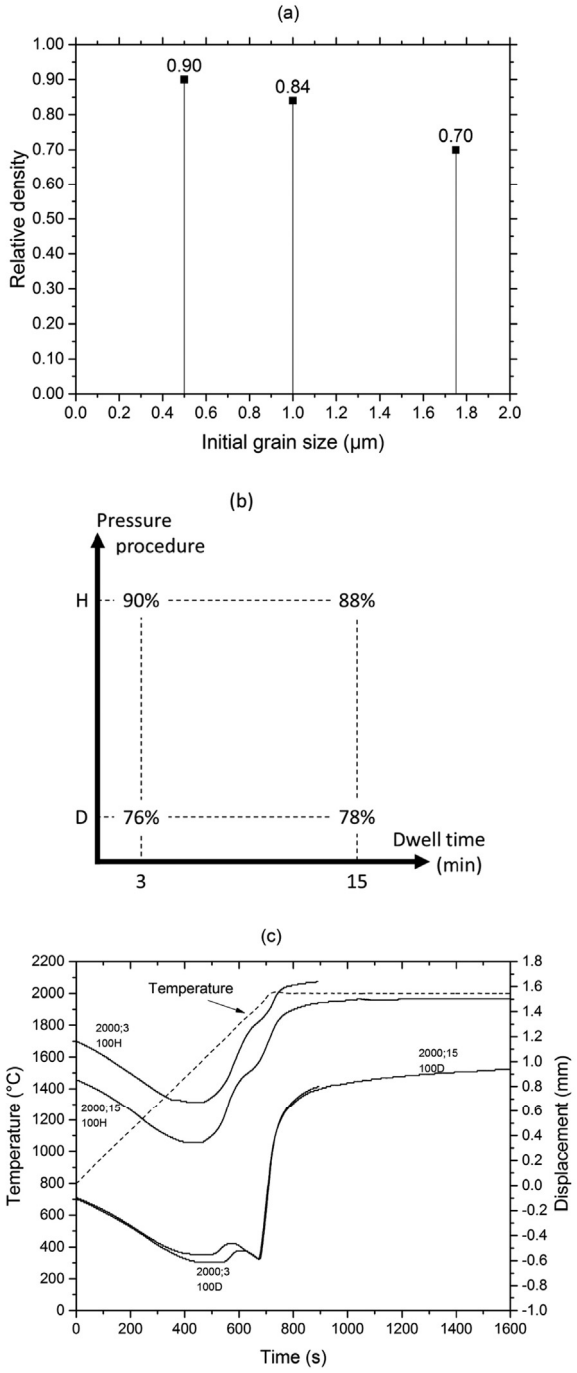

Fig. 3. (a) Size effect on SiC processed with the $\frac{2000;3}{100H}$ SPS process. (b) Pressure procedure and dwell time effect on the relative density of 0.5SiC processed at 2000 °C. (c) Densification curves of 0.5SiC for different SPS parameters.

reveals that the densification rate is very slow (dilatation of tools balances densification), regardless of the pressure procedure. This result is in agreement with Fig. 3-b. The samples using the "D" procedure present an increase in displacement higher than that of the "H" sample (Fig. 3-c) because the pressure is applied when the densification occurs. However, the total displacement is lower. It is clear that the "H" procedure is better than the "D" procedure is. This result is in conflict with a previous article on the SiC densification by SPS [27], which presents better density values when the ultimate pressure is applied at the final temperature instead of 1000 °C. This difference could be due to a higher initial pressure of 50 MPa (instead of the 0.6 MPa used in this study)

Table 1
Relative density of pure TiB_2.

Sample	Relative density (%)
$4.\ 75TiB_2{}^{2000;3}_{100H}$	83
$4.\ 75TiB_2{}^{2100;3}_{100H}$	85
$4.\ 75TiB_2{}^{2000;3}_{100D}$	86
$3TiB_2{}^{2000;3}_{100H}$	87
$3TiB_2{}^{2000;15}_{100H}$	86
$3TiB_2{}^{2000;15}_{100D}$	86
$3TiB_2$+33wt. % $4.\ 75TiB_2{}^{2000;3}_{100H}$	80
$3TiB_2$+67wt. % $4.\ 75TiB_2{}^{2000;3}_{100H}$	78

[27], which could be sufficient to ensure higher initial compaction (i.e., higher green relative density) at low temperatures and therefore optimal sintering at higher temperatures.

Finally, the densification of silicon carbide by SPS requires temperatures above 1900 °C for micron-sized powders. For submicron-sized powders, a dwell time of 3 min is sufficient. It is preferable to apply the pressure at the beginning of the cycle instead of at the final temperature. The particle size of the initial powder is a key parameter for enhancing the densification of silicon carbide using the SPS process.

3.2. Densification process of TiB_2

The two TiB_2 powders (4.75 μm and 3 μm mean size) were processed by SPS with different cycles. In addition, mixtures of these powders are also used. Table 1 shows the relative density of the pure TiB_2 samples. Increasing the temperature from 2000 °C to 2100 °C has a very slight effect on the relative density (83% and 85%, respectively). It is supposed that the densification temperature of TiB_2 micron-sized powders is lower than 2100 °C, which is in agreement with previous studies [18–21]. If the ultimate pressure is applied at the dwell time ("D"), the final relative density is better than that when the pressure is applied at 600 °C ("H"). For example, relative density increases from 83% to 86% for 4.75 TiB_2. In fact, an amorphous B_2O_3 layer covers the surface of the TiB_2 powder [32]. B_2O_3 melts at 510 °C and vaporizes approximately 2020 °C [33]. The dwell temperature is set at 2000 °C in all experiments (except one) but the SPS process is performed under vacuum (approximately 30 Pa), which means that the vaporization of B_2O_3 occurs approximately 1350 °C (value calculated by using latent heat of vaporization of 372 kJ/mol [34]). If the final pressure is applied before vaporization of B_2O_3 (samples "H"), the evacuation of boron oxide is impeded and leads to lower relative density. When the initial size of powder decreases from 4.75 μm to 3 μm, the relative density increases from 83% to 87% as expected. This difference is attributed to the finer powder having a better reactivity. In addition, two mixtures of $4.75TiB_2$ and $3TiB_2$ were processed (with 1/3 and 2/3 by weight of $4.75TiB_2$ in $3TiB_2$, respectively). These mixed samples were processed with the $\frac{2000;3}{100H}$ SPS process, and the relative densities are presented on Table 1. As shown, mixing TiB_2 of different sizes is detrimental to densification, with lower densities than those of pure $3TiB_2$ or $4.75TiB_2$.

The $4.75TiB_2$ samples and powder were analyzed by XRD. The initial powder presents some TiB impurities, but the densified samples do not. According to the Ti-B phase diagram, if the temperature inside the sample reach 2200 °C, TiB decomposes into liquid and TiB_2 (TiB is a peritectic compound) [35]. During cooling, the high quantity of TiB_2 grains could act as nucleation sites to form TiB_2 from liquid. Even if the temperature is set to 2000 °C or 2100 °C, it is known that the temperature gradients are up to 150 °C between the surface and the core of the sample during the SPS process [36–38]. Contrary to this result, Mukhopadhyay et al. found that the SPS process can lead to the formation of TiB at temperatures as low as 1400 °C from an initial TiB_2 powder free of this phase [19]. The authors investigated this

phenomenon by thermodynamic calculations and found that TiB impurities could come from (i) oxidation of TiB_2 with O_2 (even in high vacuum) and (ii) from the reaction between TiB_2, TiO_2 and free carbon [19]. However, data on SPS processing of Mukhopadhyay's powder at 2000 °C are not available [19]. The full width at half maximum, FWHM, of the main diffraction peak (approximately 44.3° in 2θ) reveals a higher value for the sample processed at 2100 °C (0.470°) than those of samples sintered at 2000 °C (0.162° and 0.251°). Broadening of the XRD peak could come from a size effect or from disordering in the crystal structure [39]. However, considering that the size effect is negligible at the micron scale [40], the difference in FWHM values is due to more crystal defects when the sintering temperature is higher. Defects in the crystal structure are mainly due to the SPS process, considering that the FWHM of the main peak for 4.75TiB_2 powder (0.070°) is close to the instrumental line profile (0.071°, from a LaB_6 sample).

Finally, the maximum density of 87% is obtained with 3TiB_2, and very high temperatures (2100 °C) do not improve the density. Therefore, additives are necessary to achieve higher relative densities with this powder.

3.3. Densification process of TiB_2-SiC

Silicon carbide is an effective additive to improve the densification rate of titanium diboride [23]. The TiB_2-SiC phase diagram presents a unique eutectic point at 2190 °C for 52 wt% SiC, and no liquid phase is expected below this temperature [41]. To improve the relative density of 3TiB_2, 0.5SiC powder was used at 2.5 wt% and 5 wt%, and the mixtures were processed by the $\frac{2000;3}{100H}$ SPS cycle (hereafter, these samples are named TS2.5 and TS5, respectively). These amounts are sufficient to ensure an improvement in the relative density [23] and adequately low to not impede the high-temperature strength [24]. Fig. 4 shows the densification results of TiB_2-SiC composites. Without the additives, the relative density of 3TiB_2 is 87%. Introducing 2.5 wt% SiC greatly enhances the densification at 97%. At higher amounts (5 wt % SiC), the relative density does not increase. These results are in good agreement with those proposed by Torizuka et al. [23]. Fig. 5 presents the XRD diagrams and MEB observations of TS2.5 and TS5. In addition, MEB observations of $3TiB_2\,\frac{2000;3}{100H}$ and $0.5SiC\,\frac{2000;3}{100H}$ are given. The XRD patterns of TS2.5 and TS5 are similar, with a main phase of titanium diboride, a secondary phase of β-SiC and some impurities of α-SiC and carbon, which is in agreement with phase composition of initial powders. The XRD patterns do not reveal significant reactions between TiB_2 and SiC. The FWHM of the main XRD peak (approximately 44.3° in 2θ) are 0.070° and 0.110° for TS2.5 and TS5, respectively. The peak

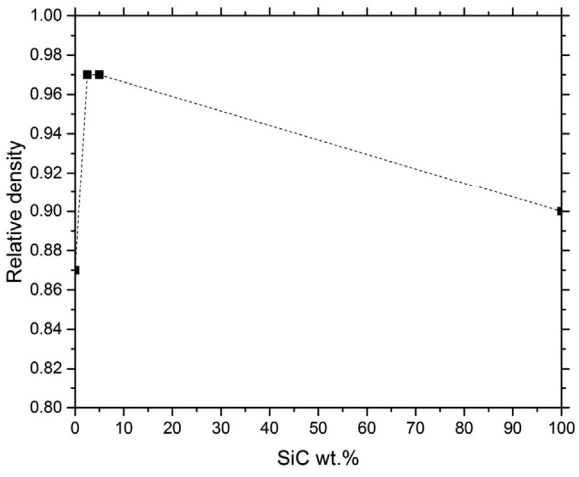

Fig. 4. Relative densities of 3TiB_2 with different amounts of 0.5SiC processed with the $\frac{2000;3}{100H}$ SPS cycle.

broadening comes from crystal defects. The FWHM of TS5 is similar to the FWHM of $3TiB_2\,\frac{2000;3}{100H}$ (0.139°), and the FWHM of TS2.5 is rather close to the FWHMs of the 3TiB_2 powder (0.081°) and instrumental line profile (0.071°). Thus, there are fewer crystal defects in TiB_2 when it is processed with 2.5 wt% SiC than with 5 wt%. The SEM observations (Fig. 5a–b) show a highly dense surface with some grain pullout due to the polishing. Particles larger than 10 μm are observed, meaning that a significant grain growth occurs during the SPS process using the TiB_2-SiC composite, probably due to the high temperature used (2000 °C). Mixing a small amount of SiC with TiB_2 is a very effective way to improve the density of both materials, as demonstrated by the SEM observations of pure 3TiB_2 and 1.75SiC (Fig. 5(c) and (d), respectively), compared to that of TS2.5 and TS5 (Fig. 5(a) and (b), respectively).

3.4. Mechanical properties

Fig. 6a presents the hardness as a function of the pore volume fraction for SiC and TiB_2 pellets. The hardness varies from 4.5 to 19.9 GPa for SiC and from 9.1 to 20.9 GPa for TiB_2. The dependence of hardness on the pore volume fraction has also been plotted for SiC [2] and TiB_2 [10] using power and exponential analytical expressions described by Eqs. (2) and (3), respectively. Eq. (3) is obtained from near-dense TiB_2 (> 96%) and is valid for 10 μm grain size and a load of 10 N (however, variations due to grain size or applied load is slight) [10] (from Snead et al. [2], Munro [10]).

$$H_{SiC}(GPa) = 27.7\times\exp(-5.4\times V_p) \quad (2)$$

$$H_{TiB_2}(GPa) = 23\times(1-V_p)^{4.1} \quad (3)$$

Where H_{SiC} and H_{TiB_2} are the hardness of TiB_2 and SiC, respectively (GPa), and V_p is the pore volume fraction. Eqs. (2) and (3) are shown in Fig. 6a.

The hardness of full-dense SiC in the literature is approximately 21–29 GPa [2]. Eq. (2) well fits the hardness of the 1.75SiC samples. The hardness values of porous SiC are scarce in the literature. However, the hardness of pressureless sintered SiC up to a porosity of 20% [42] was previously studied, and similar values (e.g., 7.4 GPa for V_p = 20%, compared to 5.7 GPa for V_p = 22% for 0.5SiC) were obtained. For the more porous silicon carbide (V_p = 33%), a hardness value of 4.1 GPa is reported [43], which is in agreement with the measured value (1.75SiC, V_p = 34%, H = 4.5 GPa). The initial particle size of silicon carbide powder has no influence on the hardness after SPS, as shown on Fig. 6a for the three particle sizes tested.

The hardness value of 3TiB_2 is remarkably higher than that of 4.75TiB_2 (roughly two times higher). However, the high scattering in the measurement appears to reveal a heterogeneous sample surface for 3TiB_2 and make the discussion of this result difficult. Mixtures of TiB_2 present a higher hardness than that of pure 4.75TiB_2, even with lower density values. The hardness value of full-dense TiB_2 (> 98%) is reported at 22–28 GPa in several works [10,44–49]. The hardness in the present study appears to be in agreement with the values from Eq. (3), even if this equation has been built by Munro without the hardness values of TiB_2 with a relative density lower than 90% [10]. In fact, data on porous TiB_2 are scarce, and there are no results on pure and porous TiB_2 (other than the values in this article). A hardness value of 10.5 GPa is reported for a TiB_2 sample with a relative density of 80.3% and 2.5 wt % Si_3N_4 [50], which is slightly lower than the value presented in this work (12.4 GPa at 80% relative density for a mixture of TiB_2). This difference should come from the softening of the grain boundaries due to the formation of amorphous SiO_2 with Si_3N_4 as a sinter-aid [47]. Using 2.5 wt% of Ti as a sinter-aid, hardness values of 13.7 and 23.8 GPa for relative densities of 62.6% and 87.6%, respectively, are measured [51]. The result at 87.6% relative density remains within the error bars of 3TiB_2, which presents a similar relative density. At lower relative density (62.6%), the reported hardness of 13.7 GPa [50] is

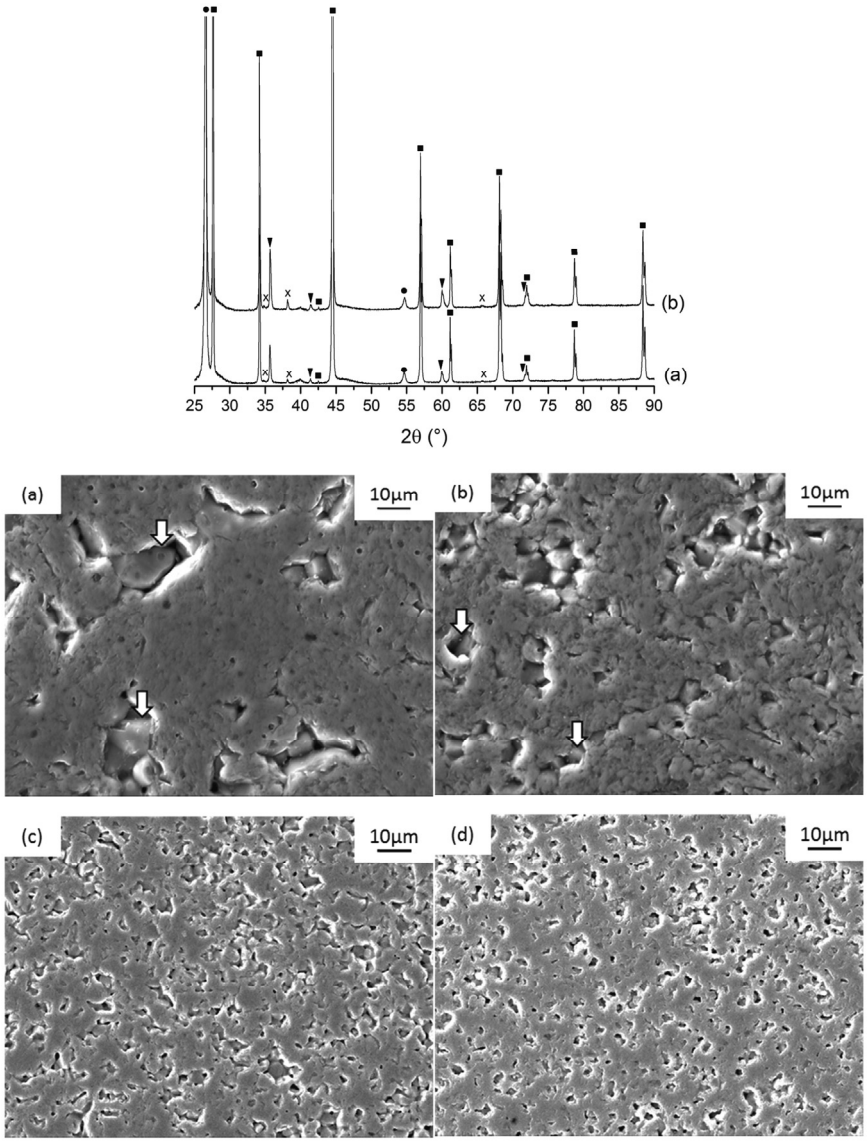

Fig. 5. XRD patterns and MEB observations of (a) TS2.5, (b) TS5, (c) 3TiB2 and (d) 0.5SiC processed by $\frac{2000;3}{100H}$ SPS cycle. Arrows show grain pullout. • Graphite (056-0159), ■ TiB2 (035-0741), ▼ 3C SiC (029-1131), × 4H SiC (029-1127).

better than those measured in this study (approximately 11.5 GPa for 79% relative density). This difference is deemed to come from grain growth inhibition due to the presence of Ti [48]. Using silicon carbide as s sinter-aid for $3TiB_2$ increases the hardness value from 18 GPa (pure TiB_2) to 19 GPa (2.5% SiC) and 23 GPa (5% SiC). The hardness value increases are mainly due to higher relative densities (97% for TS2.5 and TS5 compared to 87% for pure TiB_2 processed with the same SPS cycle). The hardness of TiB_2-SiC composites with SiC amounts lower than 10 wt% SiC was not previously studied. However, 23 GPa for TS5 is a significantly high hardness value, considering that it is in the same range as that of TiB_2 with 10–15 wt% SiC (lower values were expected because of the higher hardness of SiC) [52,53].

Fig. 6b presents the elastic modulus as a function of the pore volume fraction for SiC and TiB_2 pellets. As previously shown, the elastic modulus dependence of SiC [2] and TiB_2 [7] on the pore volume fraction can be described by the following exponential expressions (Eqs. (4) and (5)) (from Snead et al. [2], Mandorf et al. [7]).

$$E_{SiC}(GPa) = 460 \times exp\,(-3.57 \times V_p) \quad (4)$$

$$E_{TiB_2}(GPa) = 538 \times exp\,(-3.74 \times V_p) \quad (5)$$

Where E_{SiC} and E_{TiB_2} are Young's moduli (GPa) of TiB_2 and SiC, respectively, and V_p is the pore volume fraction. The values of the parameters in Eqs. (4) and (5) were obtained from a review on SiC properties [2] and from three hot-pressed TiB_2 samples [7]. Eqs. (4) and (5) are reported in Fig. 5b.

In this study, the Young's modulus values of silicon carbide vary from 148 to 277 GPa. As expected, the value strongly decreases as the pore volume fraction increases. 0.5SiC has lower Young's modulus values than do 1SiC and 1.75SiC. This difference does not come from the initial particle size because it has been shown in the literature that Young's modulus of SiC is not dependent on the grain size [2]. However, small impurities are detrimental to Young's modulus. In 0.5SiC, there is nearly double the amount of impurities (mainly free Si and oxides) compared to that in 1.75SiC (according to the supplier's data), which explains the difference in Young's modulus. For TiB_2 and SiC, the SPS parameters have no effect on Young's modulus, excluding the indirect effect of the pore volume fraction.

In this study, the Young's modulus values of TiB_2 vary from 261 to 314 GPa. For a given pore volume fraction, the Young's modulus values of $3TiB_2$ appear to be slightly lower than those of $4.75TiB_2$. A size effect

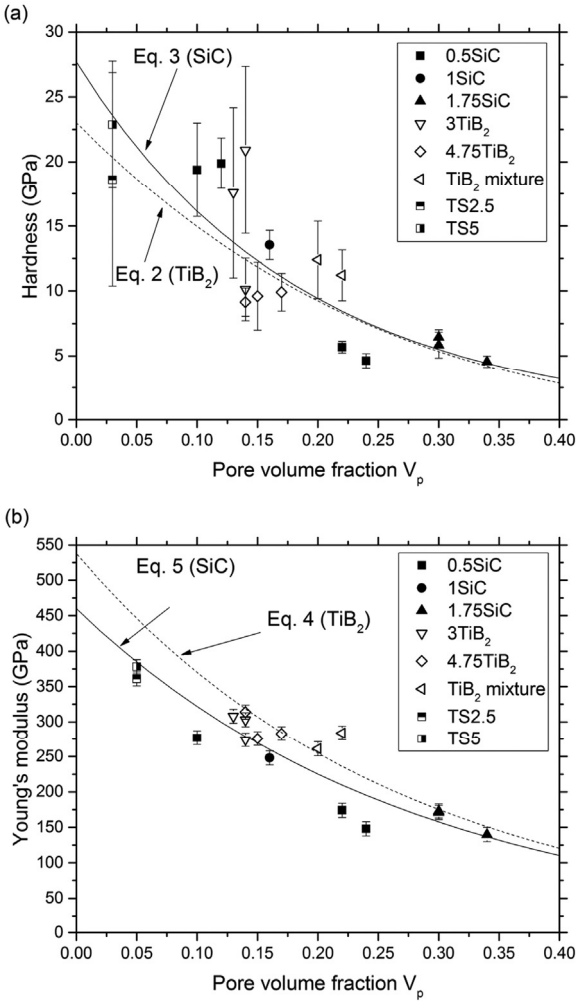

Fig. 6. (a) Hardness and (b) Young's modulus values of SiC and TiB_2 as a function of pore volume fraction.

on the elastic properties is not expected, but the $3TiB_2$ has more impurities (mainly oxides) than those of $4.75TiB_2$, according to the supplier's data, which can explain this slight difference. A mixture of 1/3 $3TiB_2$ and 2/3 $4.75TiB_2$ presents the highest Young's modulus value due to its pore volume fraction. The chosen value of Young's modulus for a full-dense TiB_2 in Eq. (5) is 538 GPa [7], which is somewhat lower than the measurements on polycrystalline TiB_2 (545–578 GPa) [10,54,55]. However, this equation fits the data well. Adding silicon carbide to the TiB_2 increases the elastic modulus value from 308 GPa (pure TiB_2) to 361 GPa (TS2.5) and 378 GPa (TS5) because of the better relative density. Considering the pore volume fraction, Young's modulus of TiB_2-SiC is lower than that of pure TiB_2. However, TS5 presents a better Young's modulus than that of TS2.5.

To summarize, the Young's modulus and hardness values of silicon carbide and titanium diboride decrease rapidly with the pore volume fraction, as expected. For example, Young's modulus of SiC is divided by 2 and its hardness by 4 when the pore volume fraction increases from 10% to 24%. The initial powder has a low influence, and the SPS parameters have no effect on the mechanical properties for a given pore volume fraction. The higher elastic modulus and hardness values are 277 GPa and 19 GPa for SiC, and 308 GPa and 21 GPa for TiB_2. The mechanical properties of a TiB_2-SiC composite with 5 wt% SiC are better than those with 2.5 wt% SiC.

4. Conclusion

Additive-free SiC, TiB_2, and composites were densified by spark plasma sintering. Densification of silicon carbide by SPS requires temperatures above 1900 °C for micron-sized powders at any dwell time and, for submicron-sized powders, a dwell time of 3 min is sufficient at 2000 °C. It is preferable to apply the pressure at the beginning of the cycle instead of at the final temperature to ensure a higher initial compaction (higher green density) at low temperatures and therefore optimal sintering at higher temperatures. The relative density of pure SiC increases continuously from 70% to 90%, while the initial particle size decreases from 1.75 μm to 0.5 μm. The maximum density achieved for pure TiB_2 is 87% at 2000 °C for 3 min. Higher temperatures do not cause the density to increase. Mixtures of different sizes of TiB_2 are detrimental to the densification process. The addition of a small amount of SiC into the TiB_2 (2.5 wt%) strongly increases the relative density from 87% to 97%. The use of higher amounts of SiC (5 wt%) does not increase the relative density. The elastic modulus and hardness are clearly related to the pore volume fraction, as expected. For a given pore volume fraction, the SPS cycle (temperature, time, and pressure procedure) has no effect on these properties. Mixtures of different sizes of TiB_2 have slightly higher Young's modulus and hardness values than those of mono-sized TiB_2. The highest Young's modulus and hardness values obtained for pure TiB_2 (relative density 86%) are 303 GPa and 21 GPa, respectively, and for pure SiC (relative density 90%), they are 277 GPa and 19 GPa, respectively. Using 5 wt% SiC in TiB_2 increases the Young's modulus and hardness values up to 378 GPa and 23 GPa, respectively, due to a higher relative density (97%). It is worth mentioning that the mechanical properties of TiB_2–5%SiC are better than those of TiB_2–2.5%SiC.

References

[1] J. Justin, A. Jankowiak, Ultra high temperature ceramics: densification, properties and thermal stability, AerospaceLab 3 (2011) 1–11.
[2] L.L. Snead, T. Nozawa, Y. Katoh, T.-S. Byun, S. Kondo, D.A. Petti, Handbook of SiC properties for fuel performance modeling, J. Nucl. Mater. 371 (2007) 329–377.
[3] C. Carter, R. Davis, J. Bentley, Kinetics and mechanisms of high-temperature creep in silicon carbide: I, reaction-bonded, J. Am. Ceram. Soc. 67 (1984) 409–417.
[4] J.E. Lane, C.H. Carter, R. Davis, Kinetics and mechanisms of high-temperature creep in silicon carbide: III, sintered α-silicon carbide, J. Am. Ceram. Soc. 71 (1988) 281–295.
[5] L. Kaufman, E.V. Clougherty, Investigation of Boride Compounds for Very High Temperature Applications, Air Force Materials Laboratory, 1965.
[6] F. Monteverde, A. Bellosi, L. Scatteia, Processing and properties of ultra-high temperature ceramics for space applications, Mater. Sci. Eng. A 485 (2008) 415–421.
[7] V. Mandorf, J. Hartwig, E.J. Seldin, High temperature properties of titanium diboride, in: G.M. Ault, W.F. Barclay, H.P. Munger (Eds.), High Temp. Mater. II, Gordon and Breach Science Publishers, 1961, pp. 455–467.
[8] J. Meléndez-Martınez, A. Domınguez-Rodrıguez, F. Monteverde, C. Melandri, G. De Portu, Characterisation and high temperature mechanical properties of zirconium boride-based materials, J. Eur. Ceram. Soc. 22 (2002) 2543–2549.
[9] A. DeGregoria, Creep and Oxidation of Hafnium Diboride-Based Ultra High Temperature Ceramics at 1500 °C, Air Force Institute of Technology, 2015.
[10] R.G. Munro, Material properties of titanium diboride, J. Res. Natl. Inst. Stand. Technol. 105 (2000) 709–720.
[11] S.-Q. Guo, Densification of ZrB_2-based composites and their mechanical and physical properties: a review, J. Eur. Ceram. Soc. 29 (2009) 995–1011.
[12] W.G. Fahrenholtz, G.E. Hilmas, I.G. Talmy, J.A. Zaykoski, Refractory diborides of zirconium and hafnium, J. Am. Ceram. Soc. 90 (2007) 1347–1364.
[13] R. Blott, C. Ferrari, G. Herdrich, Fission Nuclear Power Generation Roadmap, Disruptive Technologies ofr Space Power and Propulsion, 2013.
[14] B. Basu, G. Raju, A. Suri, Processing and properties of monolithic TiB_2 based materials, Int. Mater. Rev. 51 (2006) 352–374.
[15] M.-A. Einarsrud, E. Hagen, G. Pettersen, T. Grande, Pressureless sintering of titanium diboride with nickel, nickel boride, and iron additives, J. Am. Ceram. Soc. 80 (1997) 3013–3020.
[16] R. Orrù, R. Licheri, A.M. Locci, A. Cincotti, G. Cao, Consolidation/synthesis of materials by electric current activated/assisted sintering, Mater. Sci. Eng.: R: Rep. 63 (2009) 127–287.
[17] R. Chaim, M. Levin, A. Shlayer, C. Estournès, Sintering and densification of nanocrystalline ceramic oxide powders: a review, Adv. Appl. Ceram. 27 (2008) 159–169.
[18] Z.H. Zhang, X.B. Shen, F.C. Wang, S.K. Lee, L. Wang, Densification behavior and mechanical properties of the spark plasma sintered monolithic TiB_2 ceramics,

Mater. Sci. Eng. A 527 (2010) 5947–5951.
[19] A. Mukhopadhyay, T. Venkateswaran, B. Basu, Spark plasma sintering may lead to phase instability and inferior mechanical properties: a case study with TiB_2, Scr. Mater. 69 (2013) 159–164.
[20] A.M. Celik, R.A. Haber, K. Kuwelkar, W. Rafaniello, Preparation, characterization and development of TiB_2 hard ceramic materials, in: Wiley Online Library, Daytona Beach, Florida, 2015, pp. 131–136.
[21] A. Turan, F.C. Sahin, G. Goller, O. Yucel, Spark plasma sintering of monolithic TiB_2 ceramics, J. Ceram. Process. Res. 15 (2014) 464–468.
[22] M.M. Opeka, I.G. Talmy, J.A. Zaykoski, Oxidation-based materials selection for 2000 °C + hypersonic aerosurfaces: theorical considerations and historical experience, J. Mater. Sci., vol. 39, n.d., pp. 5887–5904.
[23] S. Torizuka, K. Sato, H. Nishio, T. Kishi, Effect of SiC on interfacial reaction and sintering mechanism of TiB_2, J. Am. Ceram. Soc. 78 (1995) 1606–1610.
[24] G. Zhao, C. Huang, H. Liu, B. Zou, H. Zhu, J. Wang, Microstructure and mechanical properties of hot pressed TiB_2–SiC composite ceramic tool materials at room and elevated temperatures, Mater. Sci. Eng. A 606 (2014) 108–116.
[25] T. Yamamoto, H. Kitaura, Y. Kodera, T. Ishii, M. Ohyanagi, Z.A. Munir, Consolidation of nanostructured β-SiC by spark plasma sintering, J. Am. Ceram. Soc. 87 (2004) 1436–1441.
[26] F. Lomello, G. Bonnefont, Y. Leconte, N. Herlin-Boime, G. Fantozzi, Processing of nano-SiC ceramics – densification by SPS and mechanical characterization, J. Eur. Ceram. Soc. 32 (2012) 633–641.
[27] F. Guillard, A. Allemand, J.-D. Lulewicz, J. Galy, Densification of SiC by SPS-effects of time, temperature and pressure, J. Eur. Ceram. Soc. 27 (2007) 2725–2728.
[28] A. Lara, A.L. Ortiz, A. Muñoz, A. Domínguez-Rodríguez, Densification of additive-free polycrystalline β-SiC by spark-plasma-sintering, Ceram. Int. 38 (45–53) (2012).
[29] S. Hayun, V. Paris, R. Mitrani, S. Kalabukhov, M.P. Dariel, E. Zaretsky, N. Frage, Microstructure and mechanical properties of silicon carbide processed by spark plasma sintering (SPS), Ceram. Int. 38 (2012) 6335–6340.
[30] B. Basu, K. Balani, Overview: high-temperature ceramics, Adv. Struct. Ceram. John Wiley & Sons, Inc., 2011, pp. 259–285.
[31] N. Tessier-Doyen, J.C. Glandus, M. Huger, Experimental and numerical study of elastic behavior of heterogeneous model materials with spherical inclusions, J. Mater. Sci. 45 (2007) 5826–5834.
[32] S. Baik, P.F. Becher, Effect of oxygen contamination on densification of TiB_2, J. Am. Ceram. Soc. 70 (1987) 527–530.
[33] A. Haddad, N. Benveniste, R. Arieli, Performance Assessments of a Boron Containing Gel Fuel Ramjet, in: Orlando, Florida, 2009.
[34] C.L. Yeh, K.K. Kuo, Ignition and combustion of boron particles, Prog. Energy Combust. Sci. 22 (1996) 511–541.
[35] J. Murray, P. Liao, K. Spear, The B–Ti (boron-titanium) system, Bull. Alloy Phase Diagr. 7 (1986) 550–555.
[36] K. Vanmeensel, A. Laptev, J. Hennicke, J. Vleugels, O. Van der Biest, Modelling of the temperature distribution during field assisted sintering, Acta Mater. 53 (2005) 4379–4388.
[37] M. Gendre, Approche des mécanismes de synthèse par carboréduction et de frittage “flash” de l’oxycarbure de zirconium, Université de Limoges, 2010.
[38] G. Maizza, S. Grasso, Y. Sakka, Moving finite-element mesh model fo aiding spark plasma sintering in current control mode of pure ultrafine WC powder, J. Mater. Sci. 44 (2009) 1219–1236.
[39] J.I. Langford, Line profiles and sample microstructure, Ind. Appl. X-Ray Diffr. Marcel Dekker, Inc., 2000, pp. 751–775.
[40] R. Guinebretiere, X-ray Diffraction by Polycrystalline Materials, Lavoisier, 2006.
[41] S. Ordan’yan, A.I. Dmitriev, E.K. Stepanenko, N.Yu Aulova, N.E. Semenov, SiC-TiB_2 system – a base of high-hardness wear-resistant materials, Powder Metall. Met. Ceram. 26 (1987) 375–377.
[42] Y.V. Milman, S.I. Chugunova, I.V. Goncharova, T. Chudoba, W. Lojkowski, W. Gooch, Temperature dependence of hardness in silicon-carbide ceramics with different porosity, Int. J. Refract. Met. Hard Mater. 17 (1999) 361–368.
[43] A.K. Gain, J.-K. Han, H.-D. Jang, B.-T. Lee, Fabrication of continuously porous SiC-Si_3N_4 composite using SiC powder by extrusion process, J. Eur. Ceram. Soc. 26 (2006) 2467–2473.
[44] J. Besson, F. Valin, P. Lointier, M. Boncoeur, Densification of titanium diboride by hot isostatic pressing and production of near-net-shape components, J. Mater. Eng. Perform. 1 (1992) 637–649.
[45] V.J. Tennery, C.B. Finch, C.S. Yust, G.W. Clark, Structure-property correlations for TiB_2-based ceramics densified using active liquid metals, in: Sci. Hard Mater., vol. 4983, pp. 891–910.
[46] R.C. Dorward, Indentation fracture of titanium diboride, J. Mater. Sci. Lett. 4 (1985) 694–696.
[47] C.E. Holcombe, N.L. Dykes, Microwave sintering of titanium diboride*, J. Mater. Sci. 26 (1991) 3730–3738.
[48] H. Itoh, S. Naka, T. Matsudaira, H. Hamamoto, Preparation of TiB_2 sintered compacts by hot pressing, J. Mater. Sci. 25 (1990) 533–536.
[49] T.S.R.C. Murthy, J. Sonber, B. Vishwanadh, A. Nagaraj, K. Sairam, R.D. Bedse, J.K. Chakravartty, Densification, characterization and oxidation studies of novel TiB_2 + EuB_6 compounds, J. Alloy. Compd. 670 (2016) 85–95.
[50] J.-H. Park, Y.-H. Lee, Y.-H. Koh, H.-E. Kim, Effect of hot-pressing temperature on densification and mechanical properties of titanium diboride with silicon nitride as a sintering aid, J. Am. Ceram. Soc. 83 (2000) 1542–1544.
[51] Z.-H. Zhang, X.-B. Shen, F.-C. Wang, S.-K. Lee, Q.-B. Fan, M.-S. Cao, Low-temperature densification of TiB_2 ceramic by the spark plasma sintering process with Ti as a sintering aid, Scr. Mater. 66 (2012) 167–170.
[52] D.S. King, W.G. Fahrenholtz, G.E. Hilmas, Silicon carbide-titanium diboride ceramic composites, J. Eur. Ceram. Soc. 33 (2013) 2943–2951.
[53] A.S. Namini, S.N.S. Gogani, M.S. Asl, K. Farhadi, M.G. Kakroudi, A. Mohammadzadeh, Microstructural development and mechanical properties of hot pressed SiC reinforced TiB_2 based composite, Int. J. Refract. Met. Hard Mater., vol. 51, n.d., pp. 169–179.
[54] H. Baumgartner, R. Steiger, Sintering and properties of titanium diboride made from powder synthesized in a plasma-arc heater, J. Am. Ceram. Soc. 67 (1984) 207–212.
[55] P.F. Becher, C.B. Finch, M.K. Ferber, Effect of residual nickel content on the grain size dependent mechanical properties of TiB_2, J. Mater. Sci. Lett. 5 (1986) 195–197.